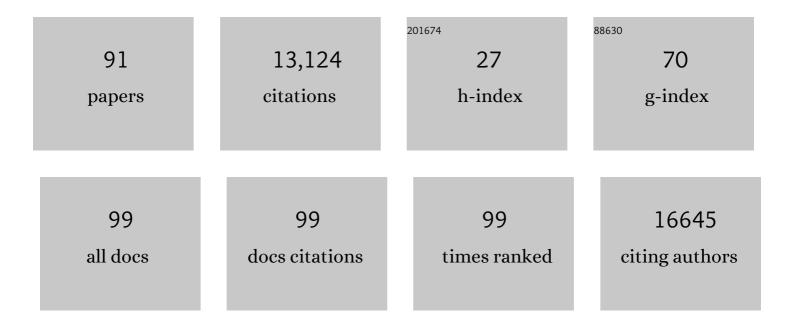
Andriy Fedorov

List of Publications by Year in descending order

Source: https://exaly.com/author-pdf/9482600/publications.pdf Version: 2024-02-01



#	Article	IF	CITATIONS
1	3D Slicer as an image computing platform for the Quantitative Imaging Network. Magnetic Resonance Imaging, 2012, 30, 1323-1341.	1.8	5,126
2	Computational Radiomics System to Decode the Radiographic Phenotype. Cancer Research, 2017, 77, e104-e107.	0.9	3,458
3	The Image Biomarker Standardization Initiative: Standardized Quantitative Radiomics for High-Throughput Image-based Phenotyping. Radiology, 2020, 295, 328-338.	7.3	1,869
4	Multiparametric MRI of prostate cancer: An update on stateâ€ofâ€theâ€art techniques and their performance in detecting and localizing prostate cancer. Journal of Magnetic Resonance Imaging, 2013, 37, 1035-1054.	3.4	192
5	GBM Volumetry using the 3D Slicer Medical Image Computing Platform. Scientific Reports, 2013, 3, 1364.	3.3	185
6	Non-rigid alignment of pre-operative MRI, fMRI, and DT-MRI with intra-operative MRI for enhanced visualization and navigation in image-guided neurosurgery. NeuroImage, 2007, 35, 609-624.	4.2	180
7	Repeatability of Multiparametric Prostate MRI Radiomics Features. Scientific Reports, 2019, 9, 9441.	3.3	169
8	Transfer Learning for Domain Adaptation in MRI: Application in Brain Lesion Segmentation. Lecture Notes in Computer Science, 2017, , 516-524.	1.3	167
9	Variations of Dynamic Contrast-Enhanced Magnetic Resonance Imaging in Evaluation of Breast Cancer Therapy Response: A Multicenter Data Analysis Challenge. Translational Oncology, 2014, 7, 153-166.	3.7	120
10	Implementing the DICOM Standard for Digital Pathology. Journal of Pathology Informatics, 2018, 9, 37.	1.7	93
11	Transperineal In-Bore 3-T MR Imaging–guided Prostate Biopsy: A Prospective Clinical Observational Study. Radiology, 2015, 274, 170-180.	7.3	75
12	The Impact of Arterial Input Function Determination Variations on Prostate Dynamic Contrast-Enhanced Magnetic Resonance Imaging Pharmacokinetic Modeling: A Multicenter Data Analysis Challenge. Tomography, 2016, 2, 56-66.	1.8	70
13	DICOM for quantitative imaging biomarker development: a standards based approach to sharing clinical data and structured PET/CT analysis results in head and neck cancer research. PeerJ, 2016, 4, e2057.	2.0	67
14	Practical considerations in T1 mapping of prostate for dynamic contrast enhancement pharmacokinetic analyses. Magnetic Resonance Imaging, 2012, 30, 1224-1233.	1.8	61
15	Increasing the impact of medical image computing using community-based open-access hackathons: The NA-MIC and 3D Slicer experience. Medical Image Analysis, 2016, 33, 176-180.	11.6	58
16	3T MR-guided in-bore transperineal prostate biopsy: A comparison of robotic and manual needle-guidance templates. Journal of Magnetic Resonance Imaging, 2015, 42, 63-71.	3.4	56
17	Multiparametric Magnetic Resonance Imaging of the Prostate. Investigative Radiology, 2017, 52, 538-546.	6.2	56
18	Errors in Quantitative Image Analysis due to Platform-Dependent Image Scaling. Translational Oncology, 2014, 7, 65-71.	3.7	51

#	Article	IF	CITATIONS
19	Image registration for targeted MRIâ€guided transperineal prostate biopsy. Journal of Magnetic Resonance Imaging, 2012, 36, 987-992.	3.4	50
20	In-bore setup and software for 3T MRI-guided transperineal prostate biopsy. Physics in Medicine and Biology, 2012, 57, 5823-5840.	3.0	46
21	The Impact of Arterial Input Function Determination Variations on Prostate Dynamic Contrast-Enhanced Magnetic Resonance Imaging Pharmacokinetic Modeling: A Multicenter Data Analysis Challenge, Part II. Tomography, 2019, 5, 99-109.	1.8	44
22	Prostate cancer discrimination in the peripheral zone with a reduced field-of-view T2-mapping MRI sequence. Magnetic Resonance Imaging, 2015, 33, 525-530.	1.8	42
23	Classification of clinical significance of MRI prostate findings using 3D convolutional neural networks. Proceedings of SPIE, 2017, 10134, .	0.8	42
24	Automatic Needle Segmentation and Localization in MRI With 3-D Convolutional Neural Networks: Application to MRI-Targeted Prostate Biopsy. IEEE Transactions on Medical Imaging, 2019, 38, 1026-1036.	8.9	42
25	A comparison of two methods for estimating DCE-MRI parameters via individual and cohort based AIFs in prostate cancer: A step towards practical implementation. Magnetic Resonance Imaging, 2014, 32, 321-329.	1.8	36
26	Open-source image registration for MRI–TRUS fusion-guided prostate interventions. International Journal of Computer Assisted Radiology and Surgery, 2015, 10, 925-934.	2.8	36
27	The Role of Pathology Correlation Approach in Prostate Cancer Index Lesion Detection and Quantitative Analysis with Multiparametric MRI. Academic Radiology, 2015, 22, 548-555.	2.5	32
28	<i>dcmqi</i> : An Open Source Library for Standardized Communication of Quantitative Image Analysis Results Using DICOM. Cancer Research, 2017, 77, e87-e90.	0.9	31
29	Toward Real-Time Image Guided Neurosurgery Using Distributed and Grid Computing. , 2006, , .		28
30	NCI Imaging Data Commons. Cancer Research, 2021, 81, 4188-4193.	0.9	28
31	DeepInfer: open-source deep learning deployment toolkit for image-guided therapy. Proceedings of SPIE, 2017, 10135, .	0.8	27
32	Diffusion-weighted endorectal MR imaging at 3T for prostate cancer: correlation with tumor cell density and percentage Gleason pattern on whole mount pathology. Abdominal Radiology, 2017, 42, 918-925.	2.1	26
33	An annotated test-retest collection of prostate multiparametric MRI. Scientific Data, 2018, 5, 180281.	5.3	26
34	Predictive role of PI-RADSv2 and ADC parameters in differentiating Gleason pattern 3 + 4 and 4 +â€ prostate cancer. Abdominal Radiology, 2019, 44, 279-285.	2.1	24
35	Quantitative pharmacokinetic analysis of prostate cancer DCE-MRI at 3T: comparison of two arterial input functions on cancer detection with digitized whole mount histopathological validation. Magnetic Resonance Imaging, 2015, 33, 886-894.	1.8	23
36	Evaluation of Brain MRI Alignment with the Robust Hausdorff Distance Measures. Lecture Notes in Computer Science, 2008, , 594-603.	1.3	22

#	Article	IF	CITATIONS
37	Multisite concordance of apparent diffusion coefficient measurements across the NCI Quantitative Imaging Network. Journal of Medical Imaging, 2017, 5, 1.	1.5	22
38	An ITK implementation of a physics-based non-rigid registration method for brain deformation in image-guided neurosurgery. Frontiers in Neuroinformatics, 2014, 8, 33.	2.5	20
39	Segmentation of prostate from ultrasound images using level sets on active band and intensity variation across edges. Medical Physics, 2016, 43, 3090-3103.	3.0	20
40	Evaluation of fitting models for prostate tissue characterization using extendedâ€range bâ€factor diffusionâ€weighted imaging. Magnetic Resonance in Medicine, 2018, 79, 2346-2358.	3.0	19
41	Towards Patient-Individual PI-Rads v2 Sector Map: Cnn for Automatic Segmentation of Prostatic Zones From T2-Weighted MRI. , 2019, , .		19
42	An Assessment of Imaging Informatics for Precision Medicine in Cancer. Yearbook of Medical Informatics, 2017, 26, 110-119.	1.0	18
43	Automatic high resolution segmentation of the prostate from multi-planar MRI. , 2018, , .		18
44	Informatics methods to enable sharing of quantitative imaging research data. Magnetic Resonance Imaging, 2012, 30, 1249-1256.	1.8	17
45	Towards Exascale Parallel Delaunay Mesh Generation. , 2009, , 319-336.		16
46	Two solutions for registration of ultrasound to MRI for image-guided prostate interventions. , 2012, 2012, 1129-32.		15
47	Co-clinical quantitative tumor volume imaging in ALK-rearranged NSCLC treated with crizotinib. European Journal of Radiology, 2017, 88, 15-20.	2.6	15
48	Parallel decoupled terminal-edge bisection method for 3D mesh generation. Engineering With Computers, 2006, 22, 111-119.	6.1	14
49	Imaging and visual analysisToward real-time image guided neurosurgery using distributed and grid computing. , 2006, , .		14
50	Atlas-Guided Segmentation of Vervet Monkey Brain MRI. Open Neuroimaging Journal, 2011, 5, 186-197.	0.2	14
51	Real-Time Non-rigid Registration of Medical Images on a Cooperative Parallel Architecture. , 2009, , .		12
52	A New Metric for Detecting Change in Slowly Evolving Brain Tumors: Validation in Meningioma Patients. Operative Neurosurgery, 2011, 68, ons225-ons233.	0.8	12
53	Probabilistic non-rigid registration of prostate images: Modeling and quantifying uncertainty. , 2011, 2011, 553-556.		12
54	Variability in MRI vs. ultrasound measures of prostate volume and its impact on treatment recommendations for favorable-risk prostate cancer patients: a case series. Radiation Oncology, 2014, 9, 200.	2.7	12

#	Article	IF	CITATIONS
55	Selection of Fitting Model and Arterial Input Function for Repeatability in Dynamic Contrast-Enhanced Prostate MRI. Academic Radiology, 2019, 26, e241-e251.	2.5	12
56	An Evaluation of Three Approaches to Tetrahedral Mesh Generation for Deformable Registration of Brain MR Images. , 0, , .		11
57	Quantitative Imaging Informatics for Cancer Research. JCO Clinical Cancer Informatics, 2020, 4, 444-453.	2.1	11
58	Multi‧ite Concordance of Diffusionâ€Weighted Imaging Quantification for Assessing Prostate Cancer Aggressiveness. Journal of Magnetic Resonance Imaging, 2022, 55, 1745-1758.	3.4	11
59	A Bayesian nonrigid registration method to enhance intraoperative target definition in imageâ€guided prostate procedures through uncertainty characterization. Medical Physics, 2012, 39, 6858-6867.	3.0	10
60	Bolus arrival time and its effect on tissue characterization with dynamic contrast-enhanced magnetic resonance imaging. Journal of Medical Imaging, 2016, 3, 014503.	1.5	10
61	Integration of patient specific modeling and advanced image processing techniques for image-guided neurosurgery. , 2006, , .		9
62	Segmented diffusion-weighted imaging of the prostate: Application to transperineal in-bore 3T MR image-guided targeted biopsy. Magnetic Resonance Imaging, 2016, 34, 1146-1154.	1.8	9
63	Multiparametric MRI as a Biomarker of Response to Neoadjuvant Therapy for Localized Prostate Cancer–A Pilot Study. Academic Radiology, 2020, 27, 1432-1439.	2.5	9
64	Tetrahedral Mesh Generation for Non-rigid Registration of Brain MRI: Analysis of the Requirements and Evaluation of Solutions. , 2008, , 55-72.		9
65	DICOM reâ€encoding of volumetrically annotated Lung Imaging Database Consortium (LIDC) nodules. Medical Physics, 2020, 47, 5953-5965.	3.0	8
66	Multi-slice-to-volume registration for MRI-guided transperineal prostate biopsy. International Journal of Computer Assisted Radiology and Surgery, 2015, 10, 563-572.	2.8	7
67	Comparison of quantitative apparent diffusion coefficient parameters with prostate imaging reporting and data system V2 assessment for detection of clinically significant peripheral zone prostate cancer. Abdominal Radiology, 2018, 43, 1237-1244.	2.1	6
68	Pathologic correlation of transperineal in-bore 3-Tesla magnetic resonance imaging-guided prostate biopsy samples with radical prostatectomy specimen. Abdominal Radiology, 2017, 42, 2154-2159.	2.1	5
69	Adaptive Physics-Based Non-Rigid Registration for Immersive Image-Guided Neuronavigation Systems. Frontiers in Digital Health, 2020, 2, 613608.	2.8	5
70	Toward uniform implementation of parametric map Digital Imaging and Communication in Medicine standard in multisite quantitative diffusion imaging studies. Journal of Medical Imaging, 2017, 5, 1.	1.5	5
71	The Effects of Young's Modulus on Predicting Prostate Deformation for MRI-Guided Interventions. , 2011, , 39-49.		4
72	The Use of Robust Local Hausdorff Distances in Accuracy Assessment for Image Alignment of Brain MRI. The Insight Journal, 2008, , .	0.2	4

#	Article	IF	CITATIONS
73	Application of Tolerance Limits to the Characterization of Image Registration Performance. IEEE Transactions on Medical Imaging, 2014, 33, 1541-1550.	8.9	3
74	Open-Source Platform for Prostate Motion Tracking During in-Bore Targeted MRI-Guided Biopsy. Lecture Notes in Computer Science, 2016, 9401, 122-129.	1.3	3
75	An ITK Implementation of Physics-based Non-rigid Registration Method. The Insight Journal, 2012, , .	0.2	3
76	A quantitative assessment of approaches to mesh generation for surgical simulation. Engineering With Computers, 2008, 24, 417-430.	6.1	2
77	Non-Rigid Registration for brain MRI: faster and cheaper. International Journal of Functional Informatics and Personalised Medicine, 2010, 3, 48.	0.4	2
78	MRI Confirmed Prostate Tissue Classification with Laplacian Eigenmaps of Ultrasound RF Spectra. Lecture Notes in Computer Science, 2012, , 19-26.	1.3	2
79	Selection of Optimal Hyper-Parameters for Estimation of Uncertainty in MRI-TRUS Registration of the Prostate. Lecture Notes in Computer Science, 2012, 15, 107-114.	1.3	2
80	Open-source Software Sustainability Models: Initial White Paper From the Informatics Technology for Cancer Research Sustainability and Industry Partnership Working Group. Journal of Medical Internet Research, 2021, 23, e20028.	4.3	2
81	Admissible subgroups of full ergodic groups. Ergodic Theory and Dynamical Systems, 1996, 16, 1221-1239.	0.6	1
82	APPLICATION-DRIVEN QUANTITATIVE ASSESSMENT OF APPROACHES TO MESH GENERATION. , 2007, , .		1
83	Location of local recurrence after MRI-guided partial prostate brachytherapy targeting only the peripheral zone: Implications for focal therapy Journal of Clinical Oncology, 2013, 31, 149-149.	1.6	1
84	Deformable Registration for IGT. , 2014, , 211-223.		1
85	Toward improved tumor targeting for image guided neurosurgery with intra-operative parametric search using distributed and grid computing. Parallel and Distributed Processing Symposium (IPDPS), Proceedings of the International Conference on, 2008, , .	1.0	Ο
86	Workflow assessment of 3T MRI-guided transperineal targeted prostate biopsy using a robotic needle guidance. , 2014, , .		0
87	Large Scale Cloud-Based Deformable Registration for Image Guided Therapy. , 2016, , .		Ο
88	Open Source Platform for Transperineal In-Bore MRI-Guided Targeted Prostate Biopsy. IEEE Transactions on Biomedical Engineering, 2020, 67, 565-576.	4.2	0
89	Grid-Enabled Software Environment for Enhanced Dynamic Data-Driven Visualization and Navigation During Image-Guided Neurosurgery. Lecture Notes in Computer Science, 2007, , 980-987.	1.3	0
90	Prototype Design and Phantom Evaluation of a Device for Co-registered MRI/TRUS Imaging of the Prostate. Lecture Notes in Computer Science, 2014, 8361, 125-133.	1.3	0

#	Article	IF	CITATIONS
91	Application of open-source computational tools to focal laser ablation of the prostate. , 2019, , .		0